

# Twenty-Five Years of Advances in Beamforming: From Convex and Nonconvex Optimization to Learning Techniques

Ahmet M. Elbir, *Senior Member, IEEE*, Kumar Vijay Mishra, *Senior Member, IEEE*,  
Sergiy A. Vorobyov, *Fellow, IEEE*, and Robert W. Heath, Jr., *Fellow, IEEE*

**Abstract**—Beamforming is a signal processing technique to steer, shape, and focus an electromagnetic wave using an array of sensors toward a desired direction. It has been used in several engineering applications such as radar, sonar, acoustics, astronomy, seismology, medical imaging, and communications. With the advances in multi-antenna technologies largely for radar and communications, there has been a great interest on beamformer design mostly relying on convex/nonconvex optimization. Recently, machine learning is being leveraged for obtaining attractive solutions to more complex beamforming problems. This article captures the evolution of beamforming in the last twenty-five years from convex-to-nonconvex optimization and optimization-to-learning approaches. It provides a glimpse of this important signal processing technique into a variety of transmit-receive architectures, propagation zones, paths, and conventional/emerging applications.

**Index Terms**—Beamforming, convexity, machine learning, radar, wireless communications.

## I. INTRODUCTION

Beamforming is ubiquitous and essential to a multitude of array processing applications such as radar, sonar, acoustics, astronomy, seismology, ultrasound, and communications (Fig. 1) [1]. Further, recent advances in mobile communications, usage of large arrays, high-frequency sensors, near-field signal recovery, and smart radio environments bring the possibility of novel signal processing problems in beamforming. These applications are driving the need for higher robustness, flexible deployment, and low complexity in beamforming algorithms and an emphasis on advanced signal processing that should be tailored for emerging application-specific requirements.

The earliest beamforming techniques are traced to the work of J. Capon during the late 1960s [2]. The key idea of the classical *Capon beamformer* is to select weight vectors or *beamformers* to minimize the array output power subjected to the linear constraint that the signal-of-interest (SOI) does

not suffer from any distortion, e.g., direction mismatch, signal fading, local scattering, etc. [2, 3]. Hence, this technique is also usually referred to as the minimum variance (MV) distortionless response (MVDR) beamforming.

The performance of Capon beamformer strongly depends on the knowledge of SOI, which is imprecise in practice because of the differences between the assumed and true array responses. The beamforming performance is usually measured by the signal-to-interference-plus-noise ratio (SINR). This may severely degrade even in the presence of small errors or mismatches in the steering vector [3]. As a result, numerous approaches have been proposed during the past decades to improve the robustness against errors/mismatches in the look direction [4, 5], array manifold [6], and local scattering [7]. These techniques are limited to only the specific mismatch they treat [8], thereby giving rise to early generalization of *robust beamforming* approaches such as sample matrix inversion (SMI) algorithm [9], robust Capon beamforming [10], eigenspace-based beamformer [11], worst-case performance optimization [8] and general-rank beamformer [12, 13].

In the late 1990s and early 2000s, significant progress was made toward robust beamformer design by exploiting *convex optimization* [14]. These methods typically consider minimizing the effect of mismatches in the array steering vectors and the look direction based on the worst-case performance optimization [8, 10, 15]. Here, the optimization problem is cast as a second-order cone (SOC) program and efficiently solved by using interior point methods. It may also be desirable to design a robust MVDR beamformer via modeling the uncertainty in the array manifold via an ellipsoid or a sphere for a particular look direction [10, 15].

During the late 2000s, certain applications of beamforming that have nonconvex objective or constraints gained salience. These included robust adaptive beamforming with additional constraints related to the positive semi-definiteness (PSD) of the signal covariance matrix [13], and the norm of the steering vectors [16–19] and stochastic distortionless response [20, 21]; multicast transmit beamforming [22], and hybrid (analog/digital) beamforming [23]. The solution to these *nonconvex optimization* problems usually requires recasting the problem into a tractable form, through the use of, for example, semi-definite relaxation (SDR), compressed sensing (CS) [23], and alternating optimization [14].

In the last decade, with the advent of the new cellular communications technologies, beamforming techniques have

A. M. Elbir is with the Interdisciplinary Centre for Security, Reliability and Trust, University of Luxembourg, Luxembourg; and the Department of Electrical and Electronics Engineering, Duzce University, Duzce, Turkey (e-mail: ahmetmelbir@gmail.com).

K. V. Mishra is with the United States DEVCOM Army Research Laboratory, Adelphi, MD 20783 USA (e-mail: kvm@ieee.org).

S. A. Vorobyov is with the Department of Signal Processing and Acoustics, Aalto University, Espoo 02150 Finland (e-mail: sergiy.vorobyov@aalto.fi).

R. W. Heath Jr. is with the Department of Electrical and Computer Engineering, North Carolina State University, Raleigh, NC 27606 USA (e-mail: rwheathjr@ncsu.edu).

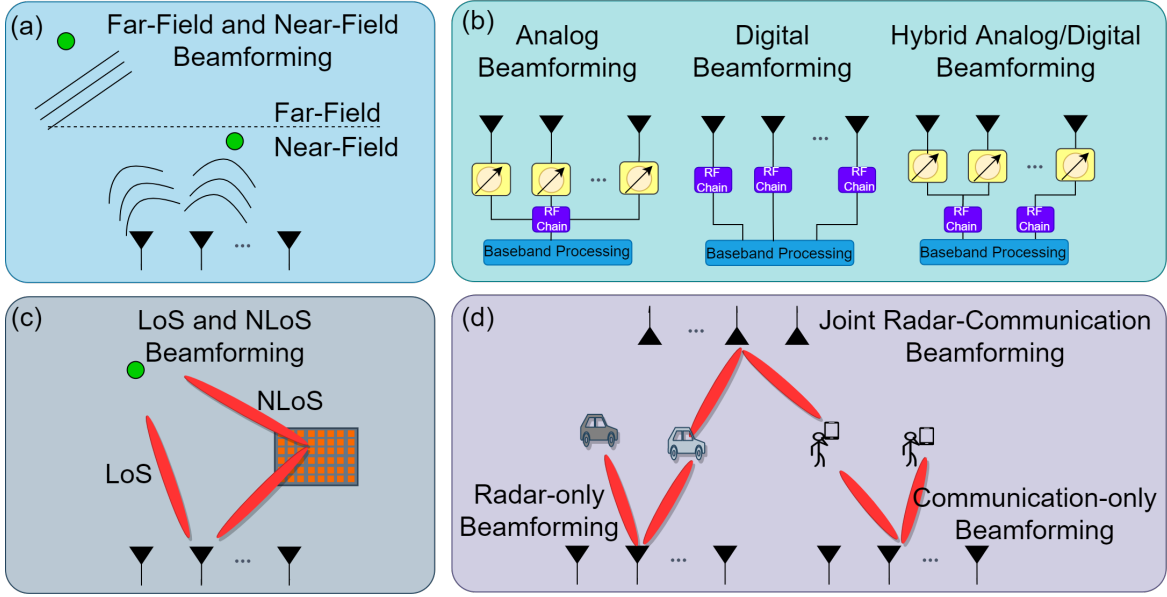


Fig. 1. Major classes of beamforming methods by (a) transmission range: far-field and near-field; (b) transceiver architectures: analog, digital, and hybrid beamforming; (c) paths: LoS and NLoS beamforming, wherein the NLoS path is controlled via joint active (transmitter) and passive (intelligent reflecting surface) devices; (d) applications: radar, communications, and joint radar-communications.

been extensively investigated for multi-antenna systems [23]. The fourth generation (4G) networks (2009-present) operating at 2.2-4.9 GHz, use fewer antennas in a multiple-input multiple-output (MIMO) configuration. However, the 5G systems (2019-present) are envisioned to employ massive number of antennas at the millimeter-wave (mm-Wave) (30-300 GHz) frequencies. This is motivated by the need to provide beamforming gain to compensate the higher path loss at mm-Wave band [24]. Furthermore, to reduce the hardware, cost, power, and area in mm-Wave massive MIMO systems, *hybrid* (analog and digital) beamforming has been introduced [23, 24]. As against a conventional digital beamformer deployed at each antenna, hybrid techniques employ large (few) number of analog (digital) beamformers to reduce the cost arising from, mainly, digital components. The hybrid beamforming is also nonconvex because of unit-modulus constraint owing to the use of phase shifters in the analog beamformers. To this end, several techniques have been developed, including sparse matrix reconstruction via CS [23], optimization over Riemannian manifolds [25], phase-extraction [26], and Gram-Schmidt orthogonalization [27].

Very recently, data-driven techniques such as *machine learning* (ML) have been leveraged to obtain beamformers. The ML is a subset of artificial intelligence (AI) that allows computers to learn directly from precedents, data, and examples without being explicitly programmed. Compared to the model-based techniques, ML has been shown to have lower post-training computational complexity, expedited design procedure, and robustness against imperfections/mismatches [28–30]. The ML-based hybrid beamforming is also envisioned to be the key to realizing massive MIMO architectures beyond 5G communications [31], such as 6G systems operating at Terahertz (THz) bands [32].

In order to shed light on the evolution of beamforming

techniques, this article presents an overview of several approaches while focusing on the major breakthroughs during the last 25 years. Specifically, the article aims at: i) highlighting the two significant leaps in this research, i.e., convex-to-nonconvex optimization, and optimization-to-learning-based beamforming; ii) depicting in detail the analytical background and the relevance of signal processing tools for beamforming, and iii) introducing the major challenges and emerging signal processing applications of beamforming.

*Notation:* Throughout this paper, uppercase and lowercase bold letters denote matrices and vectors, respectively. Also,  $(\cdot)^T$  and  $(\cdot)^H$  denote the transpose and conjugate transpose operations, respectively. For a matrix  $\mathbf{A}$ ;  $[\mathbf{A}]_{ij}$   $[\mathbf{A}]_k$ ,  $\Re\{\mathbf{A}\}$  and  $\Im\{\mathbf{A}\}$  correspond to the  $(i, j)$ -th entry,  $k$ -th column, the real and imaginary parts of  $\mathbf{A}$ , while  $\mathbf{A}^\dagger$  denotes the Moore-Penrose pseudo-inverse of  $\mathbf{A}$ , and  $\mathbf{I}$  is the identity matrix of proper size.

## II. CONVEX OPTIMIZATION FOR BEAMFORMING

Convex optimization has been employed to recast originally difficult to design beamformers to computationally attractive problems that yield exact or approximate solutions through algorithms such as interior-point methods. Its applications have traditionally transcended from simple exact Capon approach to more complex transmit, multicast, network, and distributed beamformers; see, e.g., [14] and references therein for details. In the following, we summarize the techniques that yield exact solutions. The approximate solutions are considered under nonconvex beamformers in the sequel.

### A. Capon Beamformer

Consider an antenna array with  $N$  elements. Let us define  $\mathbf{a}(\theta) \in \mathbb{C}^N$  as the array response to a plane-wave narrowband

SOI  $s(t_i)$  ( $i = 1, \dots, T$ , where  $T$  is the number of snapshots) arriving from the direction-of-arrival (DoA) angle  $\theta$ . In particular, the steering vector  $\mathbf{a}(\theta)$  is given by

$$\mathbf{a}(\theta) = \frac{1}{\sqrt{N}} [1, e^{-j2\pi \frac{d}{\lambda} \sin \theta}, \dots, e^{-j2\pi \frac{(N-1)d}{\lambda} \sin \theta}]^T, \quad (1)$$

where  $d$  is the element spacing and  $\lambda$  is the wavelength. Then, the  $N \times 1$  antenna array output is

$$\mathbf{y}(t_i) = \mathbf{a}(\theta)s(t_i) + \mathbf{e}(t_i), \quad (2)$$

where  $\mathbf{e}(t_i) \in \mathbb{C}^N$  denotes the temporarily and spatially white Gaussian noise vector with variance  $\sigma^2$ .

The received signals are multiplied by the beamforming weights i.e.,  $w_1, \dots, w_N \in \mathbb{C}$ . Therefore, the combined beamformer output becomes

$$y_o(t_i) = \mathbf{w}^H \mathbf{y}(t_i) = \mathbf{w}^H \mathbf{a}(\theta)s(t_i) + \mathbf{w}^H \mathbf{e}(t_i), \quad (3)$$

where  $\mathbf{w} = [w_1, \dots, w_N]^T$  includes the beamformer weights. In order to recover the signal  $s(t_i)$ , the beamformer weights are optimized via

$$\min_{\mathbf{w}} \mathbf{w}^H \mathbf{R}_y \mathbf{w} \quad \text{s. t. : } \mathbf{w}^H \mathbf{a}(\theta) = 1, \quad (4)$$

where  $\mathbf{R}_y = \frac{1}{T} \sum_{i=1}^T \mathbf{y}(t_i) \mathbf{y}^H(t_i)$  is the sample covariance matrix of the array output. The optimal solution for (4) is

$$\mathbf{w}_{\text{opt}} = \left( \mathbf{a}^H(\theta) \mathbf{R}_y^{-1} \mathbf{a}(\theta) \right)^{-1} \mathbf{R}_y^{-1} \mathbf{a}(\theta), \quad (5)$$

which is called Capon beamformer [2].

In order to stabilize the mainbeam response in the presence of pointing error [4], additional constrained can be added to the optimization problem as

$$\min_{\mathbf{w}} \mathbf{w}^H \mathbf{R}_y \mathbf{w} \quad \text{s. t. : } \mathbf{C}^H \mathbf{w} = \mathbf{u}, \quad (6)$$

where  $L$  many constraints are represented by  $\mathbf{C} \in \mathbb{C}^{L \times N}$  and  $\mathbf{u} \in \mathbb{C}^L$ . For example, if it is desired to maximize the beam pattern at  $30^\circ$  and place a null at  $40^\circ$ , then  $\mathbf{C} = [\mathbf{a}(30^\circ), \mathbf{a}(40^\circ)]^T$  and  $\mathbf{u} = [1, 0]^T$ . The solution to the constrained problem formulated in (6) is  $\mathbf{w}_C = \mathbf{R}_y^{-1} \mathbf{C} (\mathbf{C}^H \mathbf{R}_y^{-1} \mathbf{C})^{-1} \mathbf{u}$  [5].

### B. Loaded SMI Beamformer

Even in the ideal case, wherein the SOI direction  $\theta$  is accurately known, beamforming performance may significantly reduce due to small number of training sample size  $T$ . This can be mitigated by adding a regularization term  $\gamma$  to the objective function in (4) as

$$\min_{\mathbf{w}} \mathbf{w}^H \mathbf{R}_y \mathbf{w} + \gamma \|\mathbf{w}\|_2 \quad \text{s. t. : } \mathbf{w}^H \mathbf{a}(\theta) = 1, \quad (7)$$

which is called *loaded SMI beamforming* [9], and the solution is  $\mathbf{w}_{\text{LSMI}} = \mathbf{R}_{\text{LSMI}}^{-1} \mathbf{a}(\theta)$ , where  $\mathbf{R}_{\text{LSMI}} = \mathbf{R}_y + \gamma \mathbf{I}_N$ .

### C. Robust Capon Beamformer

The Capon beamformer in (5) requires the exact knowledge of the SOI direction  $\theta$ , which is not available in practice. Therefore, *robust beamforming* techniques have been developed to provide robustness against the inaccuracies in the estimated SOI direction and the corresponding steering vector.

A *robust* version of Capon beamforming was introduced in [10], wherein the convex optimization problem is

$$\min_{\mathbf{w}} \mathbf{w}^H \mathbf{R}_y^{-1} \mathbf{w}, \quad \text{s. t. : } \|\mathbf{w} - \bar{\mathbf{a}}\|_2 \leq \epsilon, \quad (8)$$

where  $\bar{\mathbf{a}} = \mathbf{a}(\theta + \Delta_\theta)$  is the inaccurate steering vector for mismatched direction  $\theta + \Delta_\theta$ .

### D. Beamforming With Worst-Case Performance Optimization

A more general approach is considered in [8] by taking into account the distortions in the steering vector as  $\tilde{\mathbf{a}} = \mathbf{a}(\theta) + \Delta_{\mathbf{a}}$ , where  $\Delta_{\mathbf{a}} \in \mathbb{C}^N$  represents the steering vector distortions. As a result, the optimization problem is cast based on the worst-case beamforming performance. Relying on the bounded Euclidean norm as  $\|\Delta_{\mathbf{a}}\|_2 \leq \epsilon$  corresponding to the case of spherical uncertainty [8], the following convex problem can be formulated, i.e.,

$$\min_{\mathbf{w}} \mathbf{w}^H \mathbf{R}_y \mathbf{w}, \quad \text{s. t. : } |\mathbf{w}^H \tilde{\mathbf{a}}| \geq 1, \|\Delta_{\mathbf{a}}\|_2 \leq \epsilon, \quad (9)$$

for which the LMSI-based solutions can also be obtained [3, 14]. A similar approach, called *robust MV beamforming*, has also been introduced in [15] based on ellipsoidal uncertainty model.

### E. Beamforming for General-Rank Source

In practice, the source signal is incoherently scattered such that the point-source assumption may not hold [12]. Therefore, the array covariance matrix is no longer rank-1. Therefore, instead of employing a constraint for a single steering vector, SOI covariance matrix is used. Then, the corresponding MVDR-type optimization problem becomes

$$\min_{\mathbf{w}} \mathbf{w}^H \mathbf{R}_y \mathbf{w} \quad \text{s. t. : } \mathbf{w}^H \mathbf{R}_s \mathbf{w} = 1, \quad (10)$$

where  $\mathbf{R}_s$  is SOI covariance matrix [13]. The optimal solution to (10) is  $\mathbf{w}_{\text{GR}} = \mathcal{P} [\mathbf{R}_y^{-1} \mathbf{R}_s]$ , where  $\mathcal{P} [\cdot]$  is the principal eigenvector operator.

## III. NONCONVEX BEAMFORMER DESIGN

Nonconvex beamformers [16–23, 33], tackle the design by recasting or relaxing it into tractable convex forms. This may be achieved by dropping the nonconvex constraints, or decoupling the beamforming design into multiple convex subproblems.

### A. PSD-constrained Beamforming

The general-rank beamforming solution in (10), requires the knowledge of signal covariance matrix  $\mathbf{R}_s$ , which is not always available in practice [12, 13]. Hence, the actual signal correlation matrix is modeled as  $\tilde{\mathbf{R}}_s = \mathbf{R}_s + \Delta_s$ , which is not guaranteed to be PSD in practice. In order to guarantee positive semi-definiteness of  $\tilde{\mathbf{R}}_s$ , it is first decomposed as  $\mathbf{R}_s = \mathbf{Q} \mathbf{Q}^H$ . The resulting nonconvex problem is

$$\begin{aligned} \min_{\mathbf{w}} \max_{\|\Delta_y\|_2 \leq \epsilon_y} \mathbf{w}^H (\mathbf{R}_y + \Delta_y) \mathbf{w} \\ \text{s. t. : } \min_{\|\Delta_s\|_2 \leq \epsilon_s} \mathbf{w}^H (\mathbf{Q} + \Delta_s)^H (\mathbf{Q} + \Delta_s) \mathbf{w} \geq 1, \end{aligned} \quad (11)$$

where  $\Delta_s$  and  $\Delta_y$ , whose norms are bounded by  $\varepsilon_s, \varepsilon_y$ , represent the mismatches in  $\mathbf{R}_s$  and  $\mathbf{R}_y$ , respectively. The efficient solution to the nonconvex problem in (11) is obtained via polynomial-time difference-of-convex functions (POTDC) algorithm [13].

### B. Norm-constrained Beamforming based on Steering Vector Estimation

In addition to the uncertainty constraint (8) for robust Capon beamformer [10], an additional norm constraint for the beamformer weights is considered in [16] for a more general setting as

$$\min_{\mathbf{w}} \mathbf{w}^H \hat{\mathbf{R}}^{-1} \mathbf{w} \quad \text{s. t. : } \|\mathbf{a} - \tilde{\mathbf{a}}\|_2 \leq \epsilon_a, \|\mathbf{a}\|_2^2 = N, \quad (12)$$

which is identical to (8) and convex without the constraint  $\|\mathbf{a}\|_2^2 = N$ . The nonconvex problem in (12) is called *doubly-constrained* robust Capon beamforming [16], and it is iteratively solved by interpreting it as a covariance fitting problem, while the beamforming vector is obtained via estimating the array steering vector. Robust steering vector estimation is then leading to robust beamforming. This formulation has received further development in [18], where a solution via singling out and iteratively estimating the orthogonal component of the mismatch/steering vector distortion vector has been proposed.

The solution developed in [18] has led to formulation in [19] of a new constraint that guarantees that an estimate of the source steering vector does not converge to any steering vectors of interference signals as well as their linear combinations. Then the steering vector estimation problem is formulated as

$$\min_{\hat{\mathbf{a}}} \hat{\mathbf{a}}^H \hat{\mathbf{R}}^{-1} \hat{\mathbf{a}} \quad \text{s. t. : } \|\hat{\mathbf{a}}\|_2^2 = N, \hat{\mathbf{a}}^H \tilde{\mathbf{C}} \hat{\mathbf{a}} \leq \Delta_0, \quad (13)$$

where  $\hat{\mathbf{a}} \in \mathbb{C}^N$  is the estimate of  $\mathbf{a}$  and the last constraint is the new constraint. Here,  $\tilde{\mathbf{C}} = \int_{\Theta} \mathbf{a}(\theta) \mathbf{a}^H(\theta) d\theta$  and  $\tilde{\Theta}$  is the complement of the angular sector  $\Theta = [\theta_{\min}, \theta_{\max}]$  where the desired signal is located, and  $\Delta_0$  is a uniquely selected value for a given  $\Theta$ , that is,  $\Delta_0 \triangleq \max_{\theta \in \Theta} \mathbf{a}^H(\theta) \tilde{\mathbf{C}} \mathbf{a}(\theta)$ , i.e., the boundary line to distinguish approximately whether or not the direction of  $\mathbf{a}$  is in the actual signal angular sector  $\Theta$ .

Moreover, problem (13) can be made more sophisticated as in [17], for example,

$$\begin{aligned} \min_{\hat{\mathbf{a}}} \hat{\mathbf{a}}^H \hat{\mathbf{R}}^{-1} \hat{\mathbf{a}} \quad \text{s. t. : } \hat{\mathbf{a}}^H \tilde{\mathbf{C}} \hat{\mathbf{a}} &\geq \Delta_1, \\ N(1 - \eta_1) &\leq \|\hat{\mathbf{a}}\|_2^2 \leq N(1 + \eta_2), \\ \|\mathbf{V}^H(\hat{\mathbf{a}} - \mathbf{a}_0)\|_2^2 &\leq \epsilon_u, \end{aligned} \quad (14)$$

where  $\mathbf{a}_0 = \mathbf{a}(\theta_0)$ ,  $\theta_0 = (\theta_{\max} + \theta_{\min})/2$  is the middle value of the region  $\Theta$ ,  $\mathbf{V} \in \mathbb{C}^{N \times N}$  denotes a generalized similarity constraint together with  $\mathbf{a}_0$  and  $\epsilon_u$ ,  $\mathbf{C} = \int_{\Theta} \mathbf{a}(\theta) \mathbf{a}^H(\theta) d\theta$ , and  $\Delta_1$ ,  $\eta_1$ , and  $\eta_2$  are selected values. In (14), the double-sided norm constraint accounts for gain perturbations of the steering vector and the generalized similarity condition implies that imperfect knowledge of the desired steering vector is described as in a convex set (in particular, an ellipsoidal set when  $\mathbf{V}$  is of full row rank).

All these problems are nonconvex, but can be often exactly solved through semi-definite program (SDP) relaxation, itera-

tive SOC program, QMI, and bilinear matrix inequality (BLMI) approaches.

### C. Chance-constrained Beamforming

In many applications, it is more natural that the distortionless constraint is satisfied with a certain probability. This leads to the chance-constrained robust adaptive beamforming problem [20]:

$$\min_{\mathbf{w}} \mathbf{w}^H \hat{\mathbf{R}} \mathbf{w} \quad \text{s. t. : } \Pr\{|\mathbf{w}^H \tilde{\mathbf{a}}| \geq 1\} \geq p, \quad (15)$$

where  $p$  is a certain pre-selected probability value, and  $\Pr\{\cdot\}$  stands for the probability operator. This problem corresponds to minimizing the beamformer output power subject to the *stochastic* constraint that the probability of the signal distortionless response is greater than or equal to some selected value  $p$ . The constraint can be also viewed as a *non-outage probability constraint* where the outage probability  $p_{\text{out}} = 1 - p$  is defined as that of violating the inequality  $|\mathbf{w}^H \tilde{\mathbf{a}}| \geq 1$  for random  $\tilde{\mathbf{a}}$  that consists of the presumed steering vector and the mismatch that is assumed to be random. Problem (15) is nonconvex and specified by specifying the mismatch distribution. The solutions of (15) for the case of Gaussian distributed mismatch of the signal steering vector and for the worst-case distribution are well approximated by the corresponding SOC programs [20].

A more sophisticated chance-constrained nonconvex formulation of robust adaptive beamforming is recently given in [21]. In practical scenarios, the interference-plus-noise covariance (INC) matrix  $\mathbf{R}_{i+n}$  as well as the true steering vector  $\mathbf{a}$  are not known exactly. Then considering both  $\mathbf{R}_{i+n}$  and  $\mathbf{a}$  as random variables, the following robust adaptive beamforming can be formulated, i.e.,

$$\begin{aligned} \min_{\mathbf{w}} \max_{G_1 \in \mathcal{S}_1} E_{G_1}\{\mathbf{w}^H \mathbf{R}_{i+n} \mathbf{w}\} \\ \text{s. t. : } \min_{G_2 \in \mathcal{S}_2} E_{G_2}\{\mathbf{w}^H \mathbf{a} \mathbf{a}^H \mathbf{w}\} \geq 1, \end{aligned} \quad (16)$$

where  $E_{G_1}\{\cdot\}$  ( $E_{G_2}\{\cdot\}$ ) denotes the statistical expectation under the distribution  $G_1$  ( $G_2$ ), and  $\mathcal{S}_1$  and  $\mathcal{S}_2$  are sets of distribution  $G_1$  for random matrix  $\mathbf{R}_{i+n}$  and distribution  $G_2$  for random vector  $\mathbf{a}$ , respectively. Specifically, the distribution set  $\mathcal{S}_1$  is defined in [21] as

$$\left\{ G_1 \in \mathcal{M}_1 \left| \begin{array}{l} \Pr_{G_1}\{\mathbf{R}_{i+n} \in \mathcal{Z}_1\} = 1 \\ E_{G_1}\{\mathbf{R}_{i+n}\} \succeq \mathbf{0} \\ \|E_{G_1}\{\mathbf{R}_{i+n}\} - \mathbf{S}_0\|_{\mathcal{F}} \leq \rho_1 \end{array} \right. \right\}, \quad (17)$$

where  $\mathcal{M}_1$  is the set of all probability measures,  $\mathcal{Z}_1$  is a Borel set,  $\mathbf{S}_0$  is the empirical mean of  $\mathbf{R}_{i+n}$ , that is, the sample covariance matrix  $\mathbf{R}_y$ , and  $\Pr_{G_1}\{\cdot\}$  is the probability of an event under the distribution  $G_1$ . Assuming that the mean  $\mathbf{a}_0$  and the covariance matrix  $\Sigma \succ \mathbf{0}$  of random vector  $\mathbf{a}$  under the true distribution  $\bar{G}_2$  are known, the distribution set  $\mathcal{S}_2$  is defined by

$$\left\{ G_2 \in \mathcal{M}_2 \left| \begin{array}{l} \Pr_{G_2}\{\mathbf{a} \in \mathcal{Z}_2\} = 1 \\ E_{G_2}\{\mathbf{a}\} = \mathbf{a}_0 \\ E_{G_2}\{\mathbf{a} \mathbf{a}^H\} = \Sigma + \mathbf{a}_0 \mathbf{a}_0^H \end{array} \right. \right\}, \quad (18)$$

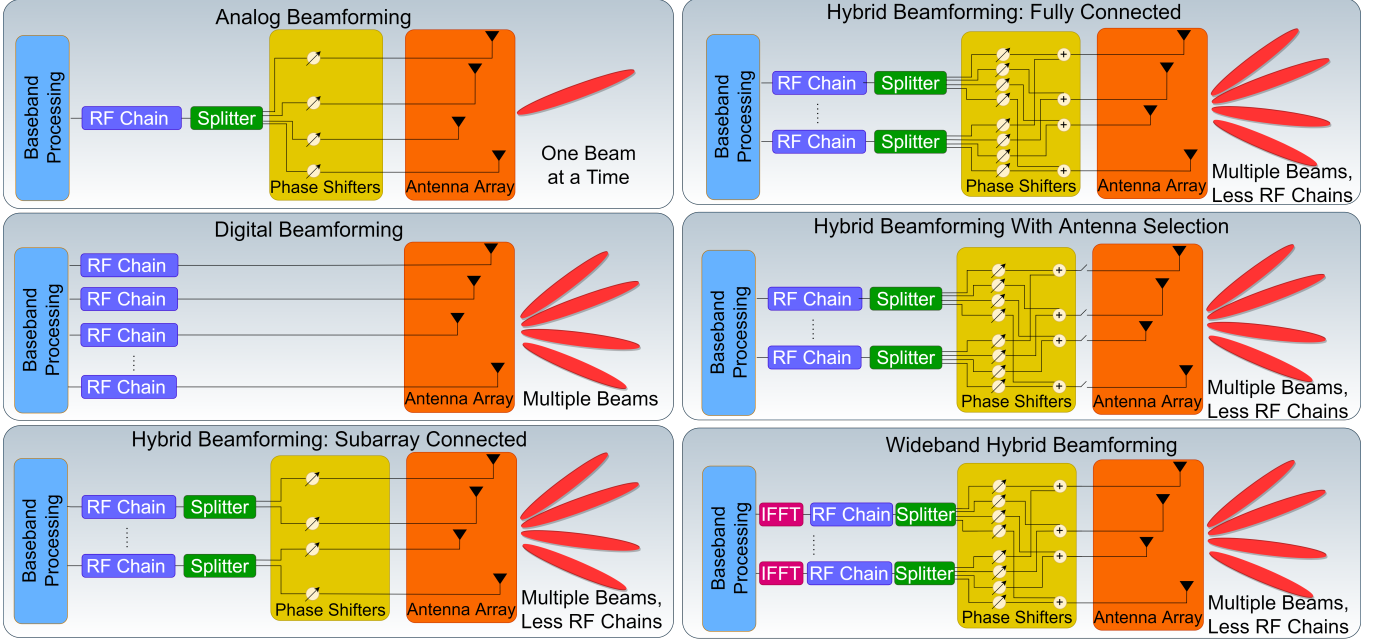


Fig. 2. Transmitter architectures for analog (Top Left), digital (Top Middle) and hybrid beamforming. While only a single beam is generated via analog beamforming (because it employs a single RF chain), multiple beams are obtained via digital beamforming but at the cost of multiple RF chains. It is possible to generate multiple beams with fewer RF chains in the *hybrid* approach through configurations such as subarray-connected (Bottom Left), fully-connected (Top Right), sparse antenna-selective (Middle Right) and wideband (Bottom Right) architectures.

where  $\mathcal{M}_2$  is the set of all probability measures and  $\mathcal{Z}_2$  is a Borel set. In other words, the set  $\mathcal{S}_2$  includes all probability distributions on  $\mathcal{Z}_2$  which have the same first- and second-order moments as  $\bar{G}_2$ . Such beamforming problem is named *distributionally robust beamforming problem* where distributional uncertainty of both the steering vector and the INC matrix are considered.

#### D. Multicast Transmit Beamforming

In communication scenario, multicast beamforming aims to broadcast data streams  $s(t_i)$  toward multiple radio receivers. In [22], a multicast beamforming technique is considered, wherein a transmitter employing  $N$ -element antenna array aims to deliver a signal to  $U$  single-antenna users. Let  $\mathbf{h}_u \in \mathbb{C}^N$  denote the wireless channel between the transmitter and the  $u$ th receiver. Then, for the beamformed transmitted signal  $\mathbf{x}(t_i) = \mathbf{w}s(t_i)$ , and the received signal at the  $u$ th user becomes

$$y_u(t_i) = \mathbf{h}_u^H \mathbf{x}(t_i) + e_u(t_i), \quad (19)$$

where  $e_u(t_i)$  denotes the noise signal with variance  $\sigma_u^2$ . Then, the multi-cast beamforming problem is

$$\begin{aligned} \min_{\mathbf{w}} \quad & \|\mathbf{w}\|_2 \\ \text{s. t.} \quad & |\mathbf{w}^H \tilde{\mathbf{h}}_u| \geq 1, \quad u \in \{1, \dots, U\}, \end{aligned} \quad (20)$$

where  $\tilde{\mathbf{h}}_u = \mathbf{h}_u / \sqrt{\rho_{\min, u} \sigma_u^2}$  is the normalized channel vector for the minimum SNR  $\rho_{\min, u}$  for the  $u$ th receiver, respectively. The optimization in (20) is quadratically constrained quadratic programming (QCQP) problem with nonconvex constraints. A rigorous solution is based on reformulating the problem using SDR. To this end, an  $N \times N$  rank-1 matrix  $\mathbf{W}$  is defined to

provide  $\mathbf{W} = \mathbf{w}\mathbf{w}^H$ . Then, the rank constrained is removed to recast problem in a convex form as

$$\min_{\mathbf{W}} \text{trace}\{\mathbf{W}\} \quad \text{s. t.} \quad \text{trace}\{\mathbf{W}\mathbf{D}_u\} \geq 1, \quad \mathbf{W} \succeq \mathbf{0}, \quad (21)$$

where  $\mathbf{D}_u = \tilde{\mathbf{h}}_u \tilde{\mathbf{h}}_u^H$ , and the beamformer weight can be obtained by using eigenvalue decomposition of  $\mathbf{W}$ . Another rigorous and more accurate solution to (20) is to write  $\mathbf{W} = \mathbf{w}_1 \mathbf{w}_2^H$ , and alternately solve for  $\mathbf{w}_1$  and  $\mathbf{w}_2$  iteratively until convergence [34].

#### E. Hybrid Analog/Digital Beamforming

Compared to analog-only and digital only-beamforming schemes, hybrid analog/digital beamforming architecture provides lower hardware cost as compared to digital beamforming while enjoying multiple beam generation as illustrated in Fig. 2. Thanks to these advantages, hybrid beamforming has become the most convenient beamforming scheme, especially for massive antenna array processing applications, e.g., 5G communication systems [24, 26].

Consider a hybrid beamforming scenario, wherein the transmitter employs  $N$  antennas and  $N_{\text{RF}}$  RF chains to send  $N_{\text{S}}$  data streams. Then, the analog and digital beamformers can be represented by  $N \times N_{\text{RF}}$  and  $N_{\text{RF}} \times N_{\text{S}}$  matrices as  $\mathbf{F}_{\text{RF}}$  and  $\mathbf{F}_{\text{BB}}$ , respectively. Here, each element of  $\mathbf{F}_{\text{RF}}$  has constant-modulus since they are realized by phase-shifters, i.e.,  $[\mathbf{F}_{\text{RF}}]_{i,j} = 1/\sqrt{N}$  for  $i = 1, \dots, N$ ,  $j = 1, \dots, N_{\text{RF}}$ . Therefore the transmitted signal becomes  $\mathbf{x} = \mathbf{F}_{\text{RF}} \mathbf{F}_{\text{BB}} \mathbf{s}$ . The hybrid beamforming problem aims to maximize mutual information  $\mathcal{I}(\mathbf{F}_{\text{RF}}, \mathbf{F}_{\text{BB}}) = \log_2 \det(\mathbf{I}_{N_{\text{S}}} + \frac{\kappa}{N_{\text{S}} \sigma_u^2} \mathbf{H} \mathbf{F}_{\text{RF}} \mathbf{F}_{\text{BB}} \mathbf{F}_{\text{BB}}^H \mathbf{F}_{\text{RF}}^H \mathbf{H}^H)$ , where  $\mathbf{H} \in \mathbb{C}^{N \times N_{\text{R}}}$  is the wireless channel matrix with  $N_{\text{R}}$  being the number of antennas

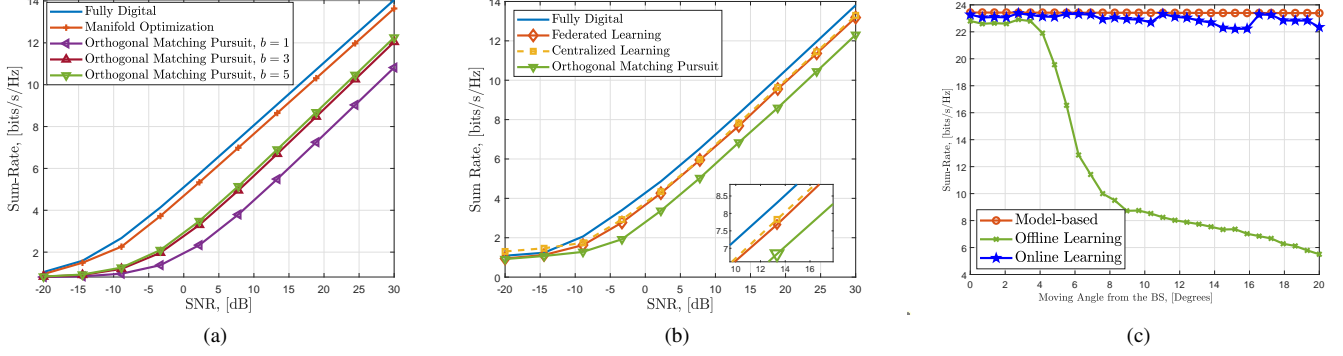


Fig. 3. Hybrid beamforming performance comparison (a) of low resolution phase shifters, and (b) of learning-based and model-based approaches in terms of sum-rate versus SNR, and (c) of offline and online learning based hybrid beamformer design. The BS has  $N = 100$  antennas, serving to  $U = 8$  users with  $N_R = 16$  antennas.

at the receiver,  $\kappa$  is the average received power and  $\sigma_n^2$  is the noise power [23]. Then, the hybrid beamforming problem becomes

$$\begin{aligned} \max_{\mathbf{F}_{\text{RF}}, \mathbf{F}_{\text{BB}}} \mathcal{I}(\mathbf{F}_{\text{RF}}, \mathbf{F}_{\text{BB}}) \quad \text{s. t. : } \|\mathbf{F}_{\text{RF}} \mathbf{F}_{\text{BB}}\|_{\mathcal{F}} = N_S, \\ |\mathbf{F}_{\text{RF}}]_{i,j}| = 1/\sqrt{N}, \end{aligned} \quad (22)$$

which is nonconvex due to constant modulus constraint, and nonlinear due to the multiplications of  $\mathbf{F}_{\text{RF}}, \mathbf{F}_{\text{BB}}$ . In order to provide an effective solution, (22) is recast to an equivalent form by minimizing the Euclidean cost between the hybrid beamformer  $\mathbf{F}_{\text{RF}} \mathbf{F}_{\text{BB}}$  and the unconstrained baseband-only beamformer  $\mathbf{F}_C \in \mathbb{C}^{N \times N_S}$  as

$$\begin{aligned} \min_{\mathbf{F}_{\text{RF}}, \mathbf{F}_{\text{BB}}} \|\mathbf{F}_{\text{RF}} \mathbf{F}_{\text{BB}} - \mathbf{F}_C\|_{\mathcal{F}} \quad \text{s. t. : } \|\mathbf{F}_{\text{RF}} \mathbf{F}_{\text{BB}}\|_{\mathcal{F}} = N_S, \\ |\mathbf{F}_{\text{RF}}]_{i,j}| = 1/\sqrt{N}, \end{aligned} \quad (23)$$

where  $\mathbf{F}_C$  can be obtained from the singular value decomposition of the channel matrix  $\mathbf{H}$  [24].

For nonconvex hybrid beamforming formulated in (23), the traditional route is to alternately optimize each ( $\mathbf{F}_{\text{RF}}$  and  $\mathbf{F}_{\text{BB}}$ ) beamformer iteratively while keeping the other one fixed [23, 25, 26]. This has been shown to provide sufficient performance in terms of spectral efficiency. Moreover, its performance is close to that of the digital-only beamformers, i.e.,  $\mathbf{F}_C$  [23, 25]. During these alternations, while estimating the digital beamformer  $\mathbf{F}_{\text{BB}}$  is straightforward as  $\mathbf{F}_{\text{BB}} = \mathbf{F}_{\text{RF}}^\dagger \mathbf{F}_C$ , the analog beamformer  $\mathbf{F}_{\text{RF}}$  is difficult to obtain. For instance,  $\mathbf{F}_{\text{RF}}$  can be formed in terms of steering vectors via CS-based techniques, wherein a dictionary of possible steering vectors are employed [23]. In MO-based approaches [25], the search space of  $\mathbf{F}_{\text{RF}}$  is regarded as a *Riemannian submanifold* of  $\mathbb{C}^N$  with a complex circle manifold.

1) *Finite Resolution Phase Shifters*: Employing continuous phase angles is expensive in practice, hence finite resolution phase shifters are used with low-resolution analog-to-digital converters (ADCs). Hence, the beamformer weights are selected from the finite set  $\mathcal{W} = \{1, \omega, \omega^2, \dots, \omega^{2^b-1}\}$ , where  $\omega = \frac{1}{\sqrt{N}} e^{j2\pi/2^b}$  and  $b$  is the number of bits. Then, the constant-modulus constraint in (23) is replaced by  $|\mathbf{F}_{\text{RF}}]_{i,j}| \in \mathcal{W}$ . A feasible solution to hybrid beamforming with finite reso-

lution is to first solve (23) under infinite resolution assumption, then quantize the phase elements of the beamformers [26].

Fig. 3(a) shows the comparison of fully digital beamforming and hybrid beamforming with low resolution phase shifters. We can see that the hybrid architecture with MO-based design provides very close performance to fully digital beamforming. Furthermore, we observe that orthogonal matching pursuit (OMP) with  $b = 5$  bit ADCs attains the closest performance to infinite resolution phase shifters while the gap from the fully digital performance is larger compared to MO-based beamforming.

2) *Wideband Hybrid beamforming*: In wideband scenario, subcarrier-dependent (SD) digital beamformers are used, and the resulting signal is transformed to the time domain via inverse fast Fourier transform (IFFT) as shown in Fig. 2. Then, subcarrier-independent analog beamformers are employed for all subcarriers. This is because the direction of the generated beam does not change significantly with respect to subcarriers in mm-Wave [24, 35]. Then, the hybrid beamforming problem for the wideband system with  $M$  subcarriers is written as

$$\begin{aligned} \min_{\mathbf{F}_{\text{RF}}, \mathbf{F}_{\text{BB}}[m]} \|\mathbf{F}_{\text{RF}} \mathbf{F}_{\text{BB}}[m] - \mathbf{F}_C[m]\|_{\mathcal{F}} \\ \text{s. t. : } \|\mathbf{F}_{\text{RF}} \mathbf{F}_{\text{BB}}[m]\|_{\mathcal{F}} = MN_S, \\ |\mathbf{F}_{\text{RF}}]_{i,j}| = 1/\sqrt{N}, \end{aligned} \quad (24)$$

where  $\mathbf{F}_{\text{BB}}[m]$  is the SD digital beamformer corresponds to the  $m$ th subcarrier,  $m \in \mathcal{M} = \{1, \dots, M\}$ .

#### IV. LEARNING-BASED BEAMFORMING

During the past few years, similar to several other signal processing applications, beamforming has also witnessed an upswing in the use of ML techniques. In learning-based hybrid beamforming scenario, the problem is approached from a model-free perspective by constructing a non-linear mapping between the input data (e.g., channel matrix, array output) and output (beamformers) of a learning model [29].

Compared to the model-based techniques, the learning-based approach has the following advantages: i) The model-free structure of the learning-based approach yields a robust performance against the corruptions/imperfections in the input



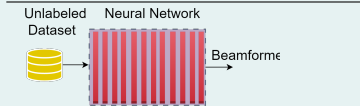
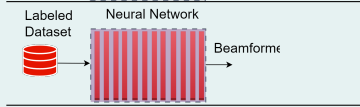
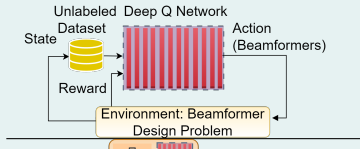
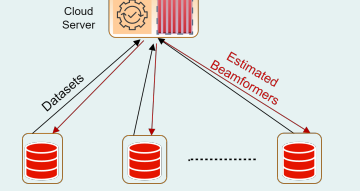
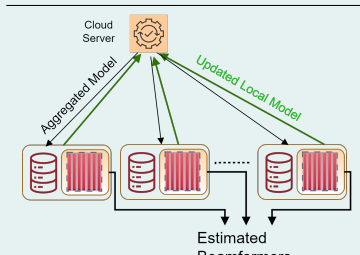
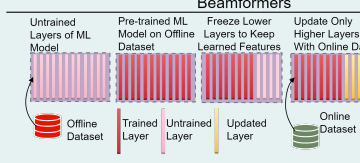
since they are data-driven. ii) Learning techniques extract feature patterns in the data. Hence, they easily update for incoming/future data, adapt in response to the environmental changes; iii) It exhibits lower computational complexity in the prediction stage than optimization. By employing parallel processing, ML significantly reduces the computation time. On the other hand, the parallel implementation of conventional optimization-based beamforming is not straightforward. Beginning from the earlier simple networks such as multi-layer perception (MLP) to more complex deep learning models like convolutional neural networks (CNNs), learning models have come a long way in successfully performing feature extraction for analog and digital beamformers [36]. Table. I summarizes various learning schemes from unsupervised/supervised learn-

ing (UL/SL) to federated learning (FL).

#### A. Unsupervised, Supervised, and Semi-Supervised Learning

The UL studies the clustering of the unlabeled data into smaller sets by exploiting the hidden features/patterns derived from the dataset, for which an answer key (label) is not provided beforehand. Hence, the “distance” between the training data samples is optimized without prior knowledge of the “meaning” of each clustered set. In SL, however, the labeled data are used for model training while minimizing the mean-squared error (MSE) between the label and the model’s response. Hence, SL is widely used for several applications of beamformer design in radar and communications [35].

TABLE I  
LEARNING SCHEMES

	<p>An unlabeled dataset is used in UL, wherein a certain optimization cost is minimized such that the beamformers are implicitly estimated via the learning model.</p>
	<p>SL-based approaches train a learning model on a labeled dataset to construct a non-linear relationship between the input and the label data (beamformers).</p>
	<p>In RL employs an unlabeled dataset, wherein the learning model learns how to design the beamformers based on a reward/punishment mechanism in accordance with optimizing the system cost.</p>
	<p>During centralized learning (CL), the training datasets are transmitted to a centralized parameter server (PS), wherein the model is trained. Once training completed, each user sends their input data to the PS, which sends back the estimated beamformers.</p>
	<p>In FL, instead of transmitting the whole dataset to the PS, each user processes its own local dataset, computes the corresponding model update, and transmits only the updates to the PS. Then, the PS broadcasts the aggregated model updates to the users, which can estimate their own beamformers.</p>
	<p>For adaptive beamforming in accordance with the deviations in the input, OL is used to update the learning model if the prediction performance degrades.</p>

Define  $\mathcal{X} \in \mathbb{R}^{N_{in}}$  and  $\mathcal{Y} \in \mathbb{R}^{N_{out}}$  as the input and label data of a learning model whose real-valued learnable parameter are stacked into vector  $\Theta \in \mathbb{R}^Q$ . Then, the relationship between the input,  $\mathcal{X} \in \mathbb{R}^{N_{in}}$  and output  $\mathcal{Y} \in \mathbb{R}^{N_{out}}$  can be represented by the nonlinear function  $f(\Theta, \mathcal{X}) : \mathbb{R}^{N_{in}} \rightarrow \mathbb{R}^{N_{out}}$ , as  $\mathcal{Y} = f(\mathcal{X}|\Theta)$ , where the input data can be designed as

the vectorized elements of the channel matrix  $\mathbf{H}$  as  $\mathcal{X} = [\text{vec}\{\Re\{\mathbf{H}\}^T, \text{vec}\{\Im\{\mathbf{H}\}^T\}]^T$ , whereas the labels include the beamforming data. In case of unit-modulus constraint, we can represent the beamformers in terms of the angle as  $\mathcal{Y} = \angle\{\mathbf{F}_{RF}\}$ . Note that the baseband beamformers can easily be obtained as  $\mathbf{F}_{BB} = \mathbf{F}_{RF}^\dagger \mathbf{F}_C$  [23].

Apart from hybrid beamforming applications, a learning-

based robust beamforming has been considered in [28]. Specifically, the sample covariance matrix is fed to a CNN whose output is the beamformer weights. In this scenario, the label data is obtained by solving the robust Capon beamformer problem in (8). During training, a dataset  $\mathcal{D} = \{\mathcal{D}_1, \dots, \mathcal{D}_J\}$  is employed, where  $\mathcal{D}_i = (\mathcal{X}_i, \mathcal{Y}_i)$  denotes the  $i$ th input-output sample for  $i = 1, \dots, J$ . Then, the model is trained by minimizing the MSE cost defined as  $\min_{\Theta} \frac{1}{J} \sum_{i=1}^J \|\mathcal{Y}_i - f(\mathcal{X}_i|\Theta)\|_2$ . Once the model is trained, the learned parameters are used for prediction purposes for beamforming. We briefly remark here recent research on employing semi-supervised learning (SSL) for acoustic beamformers [37], where both labeled and unlabeled data are used. When a small set of labeled data are available in addition to a large volume of unlabeled data, using both sets in SSL is more advantageous than SL alone.

### B. Reinforcement Learning

In RL, the learning model is initialized from a random state and the algorithms learn to react to an environment on their own [38]. The model accepts the analog and baseband beamformers of the previous state as input and then updates the model parameters by taking into account the corresponding average rate as reward. In general, RL has autonomous AI agents that gather their own data and improve based on their trial-and-error interaction with the environment. It shows a lot of promise in basic research, but so far RL has been harder to use in the real-world beamformer applications.

### C. Online Learning

The OL algorithm involves a learning model whose parameters are updated if there is a significant change in the received input data. An OL scheme for learning-based beamforming for a communication scenario is illustrated in Fig. 3(c). In this scenario, the user moves away from the BS with an increasing DoA angle. Thus, the received array data becomes different than the collected offline training data, thereby leading to poor beamforming performance. The joint hybrid beamforming and channel estimation problem is a proper choice for OL deployment since the beamformer weights are directly related to the channel matrix. In this setting [29], the model parameters are updated if the channel estimation normalized MSE (NMSE) is higher than a predetermined threshold. We can see that the learning model requires re-training in every approximately  $4^\circ$  for a massive MIMO scenario.

### D. Federated Learning

FL is more suitable for multi-user scenario. Furthermore, it mostly suits downlink beamforming, which can be performed by using the learned model available at the edge user after training. Let us assume a downlink scenario, wherein  $U$  communication users collaborate to train a model with learnable parameters  $\Theta$  with local datasets  $\mathcal{D}^{(u)} = (\mathcal{X}^{(u)}, \mathcal{Y}^{(u)})$  for  $u = 1, \dots, U$ . Here, the output data  $\mathcal{Y}^{(u)}$  involves the beamformer weights corresponding to the  $u$ th user. Then, the FL-based training problem aims optimizing  $\Theta$  such that the

averaged local cost is minimized as  $\min_{\Theta} \frac{1}{U} \sum_{u=1}^U \mathcal{L}_u(\Theta)$ , where  $i = 1, \dots, J_u$ , and  $J_u = |\mathcal{D}^{(u)}|$  denotes the number of samples in  $\mathcal{D}^{(u)}$ . Different than the cost in Section IV-A,  $\mathcal{L}_u(\Theta)$  here corresponds to the local cost  $\mathcal{L}_u(\Theta) = \frac{1}{J_u} \sum_{i=1}^{J_u} \|f(\mathcal{X}_i^{(u)}|\Theta) - \mathcal{Y}_i^{(u)}\|_2$  for the  $u$ th user. This is efficiently solved by gradient descent iteratively, wherein the model parameter update is performed at the  $t$ th iteration as  $\Theta_{t+1} = \Theta_t - \eta \frac{1}{U} \sum_{u=1}^U \beta_u(\Theta_t)$ , where  $\Theta_t$  is the computed model parameter vector at  $t$ . Here,  $\beta_u(\Theta_t) = \nabla \mathcal{L}_u(\Theta_t) \in \mathbb{R}^Q$  is the gradient vector and  $\eta$  is the learning rate. In Fig. 3(b), the hybrid beamforming performance of FL and CL is compared with model-based techniques such as orthogonal matching pursuit (OMP) and the fully digital beamformer as the benchmark in terms of sum-rate for  $U = 8$  [39]. As it is seen, both CL and FL outperform OMP, while there is a slight performance gap between CL and FL. Using the same neural network structures, CL has slightly better performance than FL since the former has access the whole dataset at once whereas the latter employs decentralized training. The performance gap between CL and FL increases with the non-uniformity of local dataset.

## V. EMERGING APPLICATIONS

Research in beamforming continues to be highly active in the light of emerging applications and theoretical advances. For example, the hybrid approach of model-driven network or deep *unfolding* for beamforming [40] allows for bounding the complexity of algorithms while also retaining their performance. Convolutional beamformers are gaining salience in acoustics [41] and ultrasound [42] as means to combine multiple, usually non-linear, operations with beamforming. Synthetic apertures across a wide variety of applications, including quantum Rydberg sensing, provide unique beamforming challenges [43]. Holographic beamformers [44] are currently investigated as attractive solutions for multi-beam steering for future wireless applications. In the following, we illustrate a few major applications in the context of radar and communications.

### A. Joint Radar-Communications

Sensing and communications systems have witnessed tremendous progress for several decades while exclusively operating in different frequency bands to minimize the interference to each other. In the last few years, there has been a substantial interest on jointly accessing the spectrum in an *joint radar and communications* (JRC) paradigm [45]. From the beamformer design perspective in JRC, we need to combine the problem settings of communication and sensing. The hybrid beamforming for communication-only problem is as given in (23). The sensing-only beamformer is modeled as  $\mathbf{F}_R \in \mathbb{C}^{N_T \times K}$ , which is actually composed of the steering vectors corresponding to the  $K$  sensing targets [35]. Then, the hybrid beamformer design problem for sensing-only system



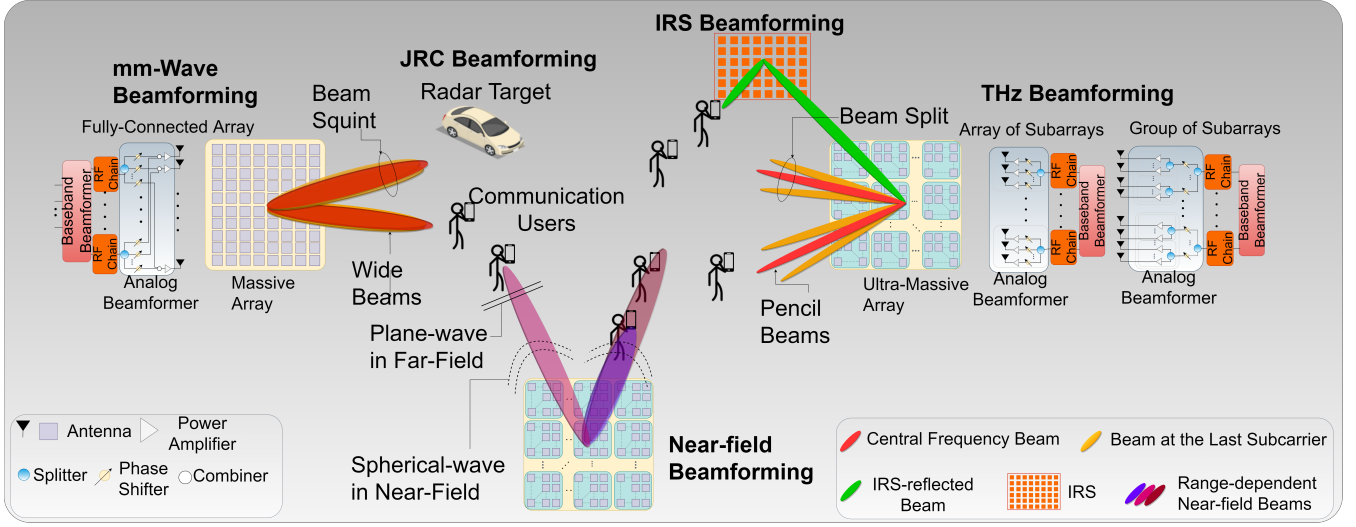


Fig. 4. In mm-Wave wideband beamforming, the generated beams are squinted, while covering the target/user, THz beamforming involves beam-split, wherein the generated beams at different subcarriers completely split into different directions. In JRC scenario, a joint optimization of beam generation toward both communication users and radar targets should be considered. Similarly, for IRS-assisted wireless systems, the beamformer weights at the transmitter and the phase shifts of the IRS elements need to be jointly designed. When the users are in the near-field region of the transmitter, range-dependent beamforming should be employed for spatial multiplexing.

can be solved, similar to (23), by minimizing the Euclidean distance between  $\mathbf{F}_{\text{RF}}\mathbf{F}_{\text{BB}}$  and  $\mathbf{F}_{\text{R}}\mathbf{P}$  as

$$\begin{aligned} \min_{\mathbf{F}_{\text{RF}}, \mathbf{F}_{\text{BB}}, \mathbf{P}} \quad & \|\mathbf{F}_{\text{RF}}\mathbf{F}_{\text{BB}} - \mathbf{F}_{\text{R}}\mathbf{P}\|_{\mathcal{F}} \\ \text{s. t.} \quad & \|\mathbf{F}_{\text{RF}}\mathbf{F}_{\text{BB}}\|_{\mathcal{F}} = N_s, \\ & |[\mathbf{F}_{\text{RF}}]_{i,j}| = 1/\sqrt{N}, \quad \forall i, j, \\ & \mathbf{P}\mathbf{P}^H = \mathbf{I}_K, \end{aligned} \quad (25)$$

where the unitary matrix  $\mathbf{P} \in \mathbb{C}^{K \times N_s}$  is an auxiliary variable to provide a change of dimension between  $\mathbf{F}_{\text{RF}}\mathbf{F}_{\text{BB}}$  and  $\mathbf{F}_{\text{R}}$  without causing any distortion in the radar beampattern.

Now, we can write the JRC hybrid beamforming problem in a compact form [35] as

$$\begin{aligned} \min_{\mathbf{F}_{\text{RF}}, \mathbf{F}_{\text{BB}}, \mathbf{P}} \quad & \|\mathbf{F}_{\text{RF}}\mathbf{F}_{\text{BB}} - \mathbf{F}_{\text{CR}}\|_{\mathcal{F}} \\ \text{s. t.} \quad & \|\mathbf{F}_{\text{RF}}\mathbf{F}_{\text{BB}}\|_{\mathcal{F}} = N_s, \\ & |[\mathbf{F}_{\text{RF}}]_{i,j}| = 1/\sqrt{N}, \quad \forall i, j, \\ & \mathbf{P}\mathbf{P}^H = \mathbf{I}_K. \end{aligned} \quad (26)$$

where we define  $\mathbf{F}_{\text{CR}} \in \mathbb{C}^{N_t \times N_s}$  as the unconstrained JRC beamformer as  $\mathbf{F}_{\text{CR}} = \zeta \mathbf{F}_{\text{C}} + (1 - \zeta) \mathbf{F}_{\text{R}}\mathbf{P}$ , where  $0 \leq \zeta \leq 1$  provides the trade-off between the radar and communication tasks.

### B. THz Communications

THz-band (0.1 – 10 THz) offers ultra-wide bandwidth and very narrow beamwidth, whereas signal processing for communication and sensing in THz-band faces several unique challenges, e.g., severe path loss due to scattering loss and molecular absorption. In order to overcome these challenges, ultra-massive antenna arrays are envisioned in different configurations, e.g., array-of-subarrays (AoSA) and group-of-subarrays (GoSA) [35] as illustrated in Fig. 4. This opens

several research opportunities for beamformer design. In order to achieve efficiency in terms of hardware and computational complexity, wideband THz systems employ a single analog beamformer for all subcarriers. However, this assumption causes the generated beams at low/high end subcarriers looking at different directions resulting *beam-split* phenomenon [35]. Meanwhile, *beam-squint* is the term commonly used for the same effect in mm-Wave, where the generated beams are squinted. As an example, the angular deviation in the beamspace due to beam-split is approximately  $6^\circ$  ( $0.4^\circ$ ) for 0.3 THz with 30 GHz (60 GHz with 1 GHz) bandwidth, respectively. While the current state-of-the-art is to use time-delayer (TD) networks to virtually realize subcarrier-dependent (SD) analog beamformers, it is possible to generate a single analog beamformer while passing the effect of beam-split into the subcarrier digital beamformers. Let us consider the analog beamformers in the problem formulated in (24), which are subcarrier-independent while the beam-split implies that the analog beamformers should be SD so that it can be mitigated. Thus, we define  $\tilde{\mathbf{F}}_{\text{BB}}[m]$  as *beam-split-aware* digital beamformer, which can be obtained via  $\tilde{\mathbf{F}}_{\text{BB}}[m] = \mathbf{F}_{\text{RF}}^H \bar{\mathbf{F}}_{\text{RF}}[m] \mathbf{F}_{\text{BB}}[m]$ , where  $\bar{\mathbf{F}}_{\text{RF}}[m]$  is the SD analog beamformer, which can be easily obtained from  $\mathbf{F}_{\text{RF}}$  for  $m \in \mathcal{M}$  [35].

### C. Intelligent Reflecting Surfaces

An intelligent reflecting surface (IRS) is composed of large number of (usually passive) meta-material elements, which reflect the incoming signal by introducing a predetermined phase shift [46]. Thus, IRS-assisted beamforming allows the BS to reach distant/blocked users/targets with less power consumption (see Fig. 4). The IRS-assisted beamforming problem involves the joint optimization of the beamformers at the BS

as well as the phase shifts of IRS elements. Consider a IRS-assisted scenario with  $N_{\text{IRS}}$  IRS elements for the BS with  $N$  antennas, the transmitted data symbol  $s \in \mathbb{C}$  is received at the user as  $y_{\text{IRS}} = (\mathbf{h}_{\text{IRS}}^H \boldsymbol{\psi} \mathbf{H}_{\text{BS}} + \mathbf{h}_{\text{D}}^H) \mathbf{f} s + e$ , where  $\mathbf{h}_{\text{IRS}} \in \mathbb{C}^{N_{\text{IRS}}}$  denotes the channel between the user and the IRS while  $\mathbf{H}_{\text{BS}} \in \mathbb{C}^{N_{\text{IRS}} \times N}$  represents the channel between the BS and the IRS. The direct channel between the user and the BS is  $\mathbf{h}_{\text{D}} \in \mathbb{C}^N$ . Here,  $\boldsymbol{\psi} = \text{diag}\{\psi_1, \dots, \psi_{N_{\text{IRS}}}\} \in \mathbb{C}^{N_{\text{IRS}} \times N_{\text{IRS}}}$  includes the IRS phase elements in a diagonal matrix, and  $\mathbf{f} \in \mathbb{C}^N$  is the beamformer vector at the BS. Finally,  $e \in \mathbb{C}$  denotes the noise signal. Then, the joint active/passive beamforming problem is formulated as

$$\begin{aligned} \max_{\boldsymbol{\psi}, \mathbf{f}} \quad & |(\mathbf{h}_{\text{IRS}}^H \boldsymbol{\psi} \mathbf{H}_{\text{BS}} + \mathbf{h}_{\text{D}}^H) \mathbf{f}|^2 \\ \text{s. t.} \quad & \|\mathbf{f}\|_2 \leq \bar{p}, \quad 0 \leq \psi_n \leq 2\pi, \end{aligned} \quad (27)$$

where  $n = 1, \dots, N_{\text{IRS}}$  and  $\bar{p}$  denotes the maximum transmit power.

### D. Near-field Beamforming

Depending on the transmission frequency, the wavefront of the transmitted signal appears to have different shapes in accordance with the observation distance. Specifically, the signal wavefront is plane-wave in the far-field while it has spherical form in the near-field (see Fig. 4) when the transmission distance is shorter than the Fraunhofer distance, i.e.,  $R_{\text{NF}} = \frac{2A^2 f_c}{c_0}$ , where  $A$  is the array aperture [47]. As a result, the near-field model is range-dependent, for which the array response vector for a ULA corresponding to the direction  $\theta$  and range  $r$  is  $\mathbf{a}(\theta, r) = \frac{1}{\sqrt{N}} [e^{-j\frac{2\pi}{\lambda} r^{(1)}}, \dots, e^{-j\frac{2\pi}{\lambda} r^{(N)}}]^T$ , where  $r^{(n)} = [r^2 + ((n-1)d)^2 - 2(n-1)dr \sin \theta]^{\frac{1}{2}} \approx r - (n-1)d \sin \theta$ , ( $n = 1, \dots, N$ ) is a range-dependent parameter between the receiver and the  $n$ th transmit antenna. The far-field signal model does not hold in the near-field because of the range-dependent term here. Hence, the beamforming should be carried out in accordance with the spherical model.

## VI. SUMMARY

The plethora of beamforming algorithms, their possible variants, and relative advantages provide a swiss-knife approach to signal processing engineers to choose the most appropriate technique for a specific application. In this context, this article presented an overview of the beamformers that had considerable impact on system design and theory during the last twenty-five years. This article focused on highlighting applications in radar and communications, while mentioning other important applications such as ultrasound, acoustics, synthetic apertures, and optics in passing.

## ACKNOWLEDGMENTS

K. V. M. acknowledges support from the U. S. National Academies of Sciences, Engineering, and Medicine via Army Research Laboratory Harry Diamond Distinguished Fellowship.

## REFERENCES

- [1] B. D. Van Veen and K. M. Buckley, "Beamforming: A versatile approach to spatial filtering," *IEEE ASSP Mag.*, vol. 5, no. 2, pp. 4–24, 1988.
- [2] J. Capon, "High-resolution frequency-wavenumber spectrum analysis," *Proc. IEEE*, vol. 57, no. 8, pp. 1408–1418, 1969.
- [3] S. A. Vorobyov, "Adaptive and robust beamforming," in *Array and Statistical Signal Processing*, ser. Academic Press Library in Signal Processing, A. M. Zoubir, M. Viberg, R. Chellappa, and S. Theodoridis, Eds. Academic Press, 2014, vol. 3, pp. 503–552.
- [4] H. Cox, "Resolving power and sensitivity to mismatch of optimum array processors," *J. Acoust. Soc. Am.*, vol. 54, no. 3, p. 771, 2005.
- [5] N. Jablon, "Adaptive beamforming with the generalized sidelobe canceller in the presence of array imperfections," *IEEE Trans. Antennas Propag.*, vol. 34, no. 8, pp. 996–1012, 1986.
- [6] A. B. Gershman, V. I. Turchin, and V. A. Zverev, "Experimental results of localization of moving underwater signal by adaptive beamforming," *IEEE Trans. Signal Process.*, vol. 43, no. 10, pp. 2249–2257, Oct. 1995.
- [7] D. Astely and B. Ottersten, "The effects of local scattering on direction of arrival estimation with MUSIC," *IEEE Trans. Signal Process.*, vol. 47, no. 12, pp. 3220–3234, 1999.
- [8] S. A. Vorobyov, A. B. Gershman, and Z.-Q. Luo, "Robust adaptive beamforming using worst-case performance optimization: A solution to the signal mismatch problem," *IEEE Trans. Signal Process.*, vol. 51, no. 2, pp. 313–324, 2003.
- [9] H. Cox, R. Zeskind, and M. Owen, "Robust adaptive beamforming," *IEEE Trans. Acoust. Speech Signal Process.*, vol. 35, no. 10, pp. 1365–1376, 1987.
- [10] J. Li, P. Stoica, and Z. Wang, "On robust Capon beamforming and diagonal loading," *IEEE Trans. Signal Process.*, vol. 51, no. 7, pp. 1702–1715, 2003.
- [11] D. D. Feldman and L. J. Griffiths, "A projection approach for robust adaptive beamforming," *IEEE Trans. Signal Process.*, vol. 42, no. 4, pp. 867–876, 1994.
- [12] S. Shahbazpanahi, A. B. Gershman, Z.-Q. Luo, and K. M. Wong, "Robust adaptive beamforming for general-rank signal models," *IEEE Trans. Signal Process.*, vol. 51, no. 9, pp. 2257–2269, Aug. 2003.
- [13] A. Khabbazi-basmenj and S. A. Vorobyov, "Robust adaptive beamforming for general-rank signal model with positive semi-definite constraint via POTDC," *IEEE Trans. Signal Process.*, vol. 61, no. 23, pp. 6103–6117, 2013.
- [14] A. B. Gershman, N. D. Sidiropoulos, S. Shahbazpanahi, M. Bengtsson, and B. Ottersten, "Convex optimization-based beamforming," *IEEE Signal Process. Mag.*, vol. 27, no. 3, pp. 62–75, 2010.
- [15] R. G. Lorenz and S. P. Boyd, "Robust minimum variance beamforming," *IEEE Trans. Signal Process.*, vol. 53, no. 5, pp. 1684–1696, 2005.
- [16] J. Li, P. Stoica, and Z. Wang, "Doubly constrained robust Capon beamformer," *IEEE Trans. Signal Process.*, vol. 52, no. 9, pp. 2407–2423, 2004.
- [17] Y. Huang, M. Zhou, and S. Vorobyov, "New designs on MVDR robust adaptive beamforming based on optimal steering vector estimation," *IEEE Trans. Signal Process.*, vol. 67, no. 14, pp. 3624–3638, 2019.
- [18] A. Hassanien, S. Vorobyov, and K. Wong, "Robust adaptive beamforming using sequential programming: An iterative solution to the mismatch problem," *IEEE Signal Process. Lett.*, vol. 15, pp. 733–736, 2008.
- [19] A. Khabbazi-basmenj, A. Hassanien, and S. Vorobyov, "Robust adaptive beamforming based on steering vector estimation with as little as possible prior information," *IEEE Trans. Signal Process.*, vol. 60, no. 6, pp. 2974–2987, 2012.
- [20] S. Vorobyov, H. Chen, and A. Gershman, "On the Relationship Between Robust Minimum Variance Beamformers With Probabilistic and Worst-Case Distortionless Response Constraints," *IEEE Trans. Signal Process.*, vol. 56, no. 11, pp. 5719–5724, Nov. 2008.
- [21] Y. Huang, W. Yang, and S. A. Vorobyov, "Robust Adaptive Beamforming Maximizing the Worst-Case SINR over Distributional Uncertainty Sets for Random INC Matrix and Signal Steering Vector," *arXiv*, Oct. 2021.
- [22] N. D. Sidiropoulos, T. N. Davidson, and Z.-Q. Luo, "Transmit beamforming for physical-layer multicasting," *IEEE Trans. Signal Process.*, vol. 54, no. 6, pp. 2239–2251, 2006.
- [23] O. E. Ayach, S. Rajagopal, S. Abu-Surra, Z. Pi, and R. W. Heath, Jr., "Spatially sparse precoding in millimeter wave MIMO systems," *IEEE Trans. Wireless Commun.*, vol. 13, no. 3, pp. 1499–1513, 2014.
- [24] R. W. Heath, Jr., N. González-Prelcic, S. Rangan, W. Roh, and A. M. Sayeed, "An overview of signal processing techniques for millimeter wave MIMO systems," *IEEE J. Sel. Top. Signal Process.*, vol. 10, no. 3, pp. 436–453, 2016.
- [25] X. Yu, J.-C. Shen, J. Zhang, and K. B. Letaief, "Alternating minimization algorithms for hybrid precoding in millimeter wave MIMO systems," *IEEE J. Sel. Top. Signal Process.*, vol. 10, no. 3, pp. 485–500, 2016.

- [26] F. Sahrabi and W. Yu, "Hybrid digital and analog beamforming design for large-scale antenna arrays," *IEEE J. Sel. Top. Signal Process.*, vol. 10, no. 3, pp. 501–513, 2016.
- [27] A. Alkhateeb and R. W. Heath, Jr., "Frequency selective hybrid precoding for limited feedback millimeter wave systems," *IEEE Trans. Commun.*, vol. 64, no. 5, pp. 1801–1818, 2016.
- [28] S. Mohammadzadeh, V. H. Nascimento, R. C. de Lamare, and N. Hajarolasvadi, "Robust Beamforming Based on Complex-Valued Convolutional Neural Networks for Sensor Arrays," *IEEE Signal Process. Lett.*, pp. 1–5, Oct. 2022.
- [29] A. M. Elbir, K. V. Mishra, M. R. B. Shankar, and B. Ottersten, "A family of deep learning architectures for channel estimation and hybrid beamforming in multi-carrier mm-Wave massive MIMO," *IEEE Trans. Cognit. Commun. Networking*, vol. 8, no. 2, pp. 642–656, 2021.
- [30] A. M. Elbir and K. V. Mishra, "Joint antenna selection and hybrid beamformer design using unquantized and quantized deep learning networks," *IEEE Trans. Wireless Commun.*, vol. 19, no. 3, pp. 1677–1688, 2019.
- [31] P. Dong, H. Zhang, and G. Y. Li, "Framework on deep learning-based joint hybrid processing for mmWave massive MIMO systems," *IEEE Access*, vol. 8, pp. 106 023–106 035, 2020.
- [32] I. F. Akyildiz, A. Kak, and S. Nie, "6G and beyond: The future of wireless communications systems," *IEEE Access*, vol. 8, pp. 133 995–134 030, 2020.
- [33] K. Roth, H. Pirzadeh, A. L. Swindlehurst, and J. A. Nossek, "A comparison of hybrid beamforming and digital beamforming with low-resolution ADCs for multiple users and imperfect CSI," *IEEE J. Sel. Top. Signal Process.*, vol. 12, no. 3, pp. 484–498, 2018.
- [34] Ö. T. Demir and T. E. Tuncer, "Alternating maximization algorithm for the broadcast beamforming," in *European Signal Processing Conference*, 2014, pp. 1915–1919.
- [35] A. M. Elbir, K. V. Mishra, and S. Chatzinotas, "Terahertz-band joint ultra-massive MIMO radar-communications: Model-based and model-free hybrid beamforming," *IEEE J. Sel. Top. Signal Process.*, vol. 15, no. 6, pp. 1468–1483, 2021.
- [36] A. M. Elbir, "CNN-based precoder and combiner design in mmWave MIMO systems," *IEEE Commun. Lett.*, vol. 23, no. 7, pp. 1240–1243, 2019.
- [37] S. Wager, A. Khare, M. Wu, K. Kumatani, and S. Sundaram, "Fully learnable front-end for multi-channel acoustic modeling using semi-supervised learning," in *IEEE International Conference on Acoustics, Speech and Signal Processing*, 2020, pp. 6864–6868.
- [38] Q. Wang, K. Feng, X. Li, and S. Jin, "PrecoderNet: Hybrid beamforming for millimeter wave systems with deep reinforcement learning," *IEEE Wireless Commun. Lett.*, vol. 9, no. 10, pp. 1677–1681, 2020.
- [39] A. M. Elbir and S. Coleri, "Federated learning for hybrid beamforming in mm-Wave massive MIMO," *IEEE Commun. Lett.*, vol. 24, no. 12, pp. 2795–2799, 2020.
- [40] S. Shi, Y. Cai, Q. Hu, B. Champagne, and L. Hanzo, "Deep-unfolding neural-network aided hybrid beamforming based on symbol-error probability minimization," *IEEE Transactions on Vehicular Technology*, 2022, in press.
- [41] T. Nakatani and K. Kinoshita, "A unified convolutional beamformer for simultaneous denoising and dereverberation," *IEEE Signal Processing Letters*, vol. 26, no. 6, pp. 903–907, 2019.
- [42] B. Heriard-Dubreuil, A. Besson, F. Wintzenrieth, J.-P. Thiran, and C. Cohen-Bacrie, "Sparse convolutional plane-wave compounding for ultrasound imaging," in *IEEE International Ultrasonics Symposium*, 2020, pp. 1–4.
- [43] P. Vouras, K. V. Mishra, A. Artusio-Glimpse, S. Pinilla, A. Xenaki, D. W. Griffith, and K. Egiiazarian, "An overview of advances in signal processing techniques for classical and quantum wideband synthetic apertures," *arXiv preprint arXiv:2205.05602*, 2022.
- [44] R. Deng, B. Di, H. Zhang, Y. Tan, and L. Song, "Reconfigurable holographic surface: Holographic beamforming for metasurface-aided wireless communications," *IEEE Transactions on Vehicular Technology*, vol. 70, no. 6, pp. 6255–6259, 2021.
- [45] K. V. Mishra, M. R. Bhavani Shankar, V. Koivunen, B. Ottersten, and S. A. Vorobyov, "Toward millimeter wave joint radar-communications: A signal processing perspective," *IEEE Signal Process. Mag.*, vol. 36, no. 5, pp. 100–114, 2019.
- [46] Q. Wu and R. Zhang, "Intelligent reflecting surface enhanced wireless network via joint active and passive beamforming," *IEEE Trans. Wireless Commun.*, vol. 18, no. 11, pp. 5394–5409, 2019.
- [47] R. A. Kennedy, T. D. Abhayapala, and D. B. Ward, "Broadband nearfield beamforming using a radial beampattern transformation," *IEEE Trans. Signal Process.*, vol. 46, no. 8, pp. 2147–2156, 1998.